

Performance of Nonlinear Dispersive APML in High-Order FDTD Schemes

Masafumi Fujii, Manos M. Tentzeris[†] and Peter Russer

Institute for High-Frequency Engineering, University of Technology Munich
Arcisstrasse 21, D-80333 Munich, Germany

[†]School of ECE, Georgia Institute of Technology, Atlanta, GA 30332-250, USA
e-mail: fujii@ei.tum.de

Abstract—A consistent reformulation of the anisotropic perfectly matched layer (APML) absorbing boundary has been presented for general nonlinear dispersive media. The APML is then adopted in the high-order finite-difference-based schemes, and improved absorption has been achieved.

Keywords—time domain electromagnetic field analysis, high-order FDTD, APML, nonlinear dispersive media

I. INTRODUCTION

Time-domain numerical techniques are of primary importance in the analysis of nonlinear pulse propagation since the principle of superposition no longer holds and frequency-domain techniques are basically inapplicable.

In order to model the linear and nonlinear dispersive response functions such as the Lorentz dispersion and the Raman effects, a z-transform technique [1], [2] and a convolution integral technique combined with a system of differential equations [3], [4], [5] have been employed. This convolution technique formulates the relation between the polarization and the electric flux density, which saves some memory with the expense of solving a system of equations. The auxiliary differential equation (ADE) technique has been applied to the formulation of the polarization current to avoid the system of equations for the linear dispersion case [6] and for a second-order nonlinear case [7].

We have implemented the nonlinear and dispersive anisotropic perfectly matched layer (APML) [8], and moreover, adopted the APML in the high-order finite-difference time-domain (FDTD) schemes of Maxwell's equations based on the biorthogonal interpolating scaling function [9]; based only on the scaling function, the scheme is equivalent to the FDTD schemes of high spatial-order derived by the Taylor series expansion.

The formulation of the material property is based on the aforementioned ADE technique with modification to polarization, and the constitutive equation in the FDTD scheme is formulated by simple modification to the original APML for lossy media [7]. In this paper, the performance of the absorption by the APML has been investigated for high-order FDTD-based schemes.

II. THEORY

A. Discretization of Maxwell's Equation for Linear and Nonlinear Dispersive Media

We start with the two-dimensional TE polarized wave propagating in the xz -plane of the Cartesian coordinates represented by Maxwell's equations

$$\frac{\partial H_x}{\partial z} - \frac{\partial H_z}{\partial x} = J_y + \frac{\partial D_y}{\partial t}, \quad (1)$$

$$-\frac{\partial E_y}{\partial z} = -\mu \frac{\partial H_x}{\partial t}, \quad (2)$$

$$\frac{\partial E_y}{\partial x} = -\mu \frac{\partial H_z}{\partial t}, \quad (3)$$

where D denotes the electric flux density, E the electric field, H the magnetic field, and J the source excitation current. In order to obtain a consistent formulation both in the APML and the normal media, contrary to the previously proposed techniques [6], [7], polarization is used to represent the dispersive and the nonlinear material properties. The constitutive equation is written as

$$D_y = \varepsilon_0 \varepsilon_\infty E_y + P_y^{(linear)} + P_y^{(nonlinear)}, \quad (4)$$

where ε_0 is the dielectric constant of free space, ε_∞ is the relative dielectric constant in the limit of infinite frequency. The linear and third-order nonlinear polarization of interest are written respectively by

$$P_y^{(linear)} = \varepsilon_0 \chi^{(1)} E_y \quad (5)$$

and

$$P_y^{(nonlinear)} = \varepsilon_0 \chi^{(3)} E_y, \quad (6)$$

where $\chi^{(1)}$ denotes the linear susceptibility and $\chi^{(3)}$ the third-order nonlinear susceptibility.

The time evolution equation of D and H is obtained by the standard Yee's leapfrog algorithm [10], i.e. for (1)

$$D_{y,i,k}^{n+1} = \frac{2\varepsilon_0 - \sigma_z \Delta t}{2\varepsilon_0 + \sigma_z \Delta t} D_{y,i,k}^n + \frac{2\varepsilon_0 \Delta t}{2\varepsilon_0 + \sigma_z \Delta t} (\delta H^{(y)} - J_{y,i,k}^{n+1/2}), \quad (7)$$

where n is the time step index, i and k are the space step indices, and the space-time discrete value of electric or magnetic field $F_\xi(x, z, t)$ for $\xi = x, y, z$ is defined by $F_{\xi, i, k}^n \equiv F_\xi(i\Delta x, k\Delta z, n\Delta t)$. Notation $\delta H^{(y)}$ is the spatial discrete derivative of the magnetic field

$$\delta H^{(y)} = \frac{H_{x, i, k+1/2}^{n+1/2} - H_{x, i, k-1/2}^{n+1/2}}{\Delta z} - \frac{H_{z, i+1/2, k}^{n+1/2} - H_{z, i-1/2, k}^{n+1/2}}{\Delta x}, \quad (8)$$

which can be replaced by the high-order finite-difference scheme or the wavelet-based schemes [11], [12]. For (2) and (3), the magnetic field is updated similarly.

B. Nonlinear Dispersive Anisotropic Perfectly Matched Layer

Starting with a constitutive relation between the flux density D_y and the electric field E_y in the medium of frequency dependent relative dielectric constant $\varepsilon_r(\omega)$, we write in the frequency domain as in [7],

$$\tilde{D}_y(\omega) = \varepsilon_0 \varepsilon_r(\omega) \tilde{E}_y(\omega). \quad (9)$$

The time-harmonic Ampère's law within the APML is written as

$$\frac{\partial \tilde{H}_x(\omega)}{\partial z} - \frac{\partial \tilde{H}_z(\omega)}{\partial x} = j\omega \varepsilon_0 \varepsilon_r(\omega) \frac{s_x s_z}{s_y} \tilde{E}_y(\omega), \quad (10)$$

where

$$s_\xi = \kappa_\xi + \frac{\sigma_\xi}{j\omega \varepsilon_0} \quad (11)$$

for $\xi = x, y$ and z . The APML parameters κ_ξ and σ_ξ normally have an polynomial grading.

We introduce now two auxiliary variables \tilde{D}_y and \tilde{E}_y defined by

$$\tilde{D}_y(\omega) = \varepsilon_0 \varepsilon_r(\omega) \frac{s_x}{s_y} \tilde{E}_y(\omega), \quad (12)$$

and

$$\tilde{E}_y(\omega) = \frac{1}{\varepsilon_0 \varepsilon_r(\omega)} \tilde{D}_y(\omega). \quad (13)$$

The variables \tilde{D}_y and \tilde{E}_y represent the equivalent flux density and the equivalent electric field in the APML loss space, respectively. Substituting (12) into (10), and applying the usual ADE procedure of the inverse Fourier transform, i.e. replacing the factor $j\omega$ with differentiation $\partial/\partial t$, we obtain

$$\frac{\partial H_x(t)}{\partial z} - \frac{\partial H_z(t)}{\partial x} = \kappa_z \frac{\partial \tilde{D}_y(t)}{\partial t} + \frac{\sigma_z}{\varepsilon_0} \tilde{D}_y(t). \quad (14)$$

Equation (14) is discretized using the semi-implicit scheme for the right hand side of the equation, yielding

$$\begin{aligned} \tilde{D}_{y, i, k}^{n+1} = & \frac{2\varepsilon_0 \kappa_z - \sigma_z \Delta t}{2\varepsilon_0 \kappa_z + \sigma_z \Delta t} \tilde{D}_{y, i, k}^n \\ & + \frac{2\varepsilon_0 \Delta t}{2\varepsilon_0 \kappa_z + \sigma_z \Delta t} \delta H^{(y)}, \end{aligned} \quad (15)$$

where $\delta H^{(y)}$ is again the spatial discrete derivative of the magnetic field (8) or the high-order counterparts.

Now the linear and nonlinear dispersive properties are implemented by the auxiliary differential equation. From (13) we can write

$$\begin{aligned} \tilde{D}_y(\omega) = & \varepsilon_0 \varepsilon_r(\omega) \tilde{E}_y(\omega) \\ = & \varepsilon_0 \varepsilon_\infty \tilde{E}_y(\omega) \\ & + \tilde{\mathcal{P}}^{(linear)}(\omega) + \tilde{\mathcal{P}}^{(nonlinear)}(\omega), \end{aligned} \quad (16)$$

where $\tilde{\mathcal{P}}^{(linear)}$ and $\tilde{\mathcal{P}}^{(nonlinear)}$ denote the linear and the nonlinear polarization in the APML loss space, respectively. By applying the inverse Fourier transform, the expression in the time domain is obtained as

$$\begin{aligned} \mathcal{D}_y(t) = & \varepsilon_0 \varepsilon_\infty \mathcal{E}_y(t) \\ & + \mathcal{P}^{(linear)}(t) + \mathcal{P}^{(nonlinear)}(t). \end{aligned} \quad (17)$$

The equivalent electric field in the APML loss space is obtained by solving the single nonlinear equation (17). Linear and/or nonlinear polarizations are in general given by the ADE technique in a recursive form, and they are to be simply substituted in (17).

Finally, from (12) and (13), we have

$$\tilde{E}_y(\omega) = \frac{s_x}{s_y} \tilde{E}_y(\omega). \quad (18)$$

Substituting (11) into (18) leads to

$$\tilde{E}_y \left(\kappa_y + \frac{\sigma_y}{j\omega \varepsilon_0} \right) = \tilde{E}_y \left(\kappa_x + \frac{\sigma_x}{j\omega \varepsilon_0} \right). \quad (19)$$

The inverse Fourier transform of (19) followed by discretization gives

$$\begin{aligned} \tilde{E}_{y, i, k}^{n+1} = & \frac{2\kappa_x \varepsilon_0 - \sigma_x \Delta t}{2\kappa_x \varepsilon_0 + \sigma_x \Delta t} \tilde{E}_{y, i, k}^n + \frac{1}{2\kappa_x \varepsilon_0 + \sigma_x \Delta t} \\ & \cdot [(2\kappa_y \varepsilon_0 + \sigma_y \Delta t) \tilde{E}_{y, i, k}^{n+1} \\ & - (2\kappa_y \varepsilon_0 - \sigma_y \Delta t) \tilde{E}_{y, i, k}^n]. \end{aligned} \quad (20)$$

To summarize, computing (15), (17) and (20) in sequence completes the update of the electric field. The magnetic fields can be updated by the standard APML algorithm for non-magnetic media. The influence of adding wavelet terms will appear in the nonlinear constitutive equations (4) and (17); note that, in the case of interpolating wavelet basis, the coupling is only unilateral from scaling to wavelet coefficients.

C. Time Discrete Equations for Nonlinear and Dispersive Polarization

For example, the linear Lorentz dispersion of an oscillating frequency ω_L , a dumping factor δ_L and a dielectric constant change $\Delta\epsilon_L$

$$\tilde{P}_L(\omega) = \frac{\epsilon_0 \Delta\epsilon_L \omega_L^2}{\omega_L^2 + 2j\omega\delta_L - \omega^2} \tilde{E}(\omega) \quad (21)$$

is implemented by the discrete recursive form as

$$P_L^{n+1} = a_L P_L^n + b_L P_L^{n-1} + c_L E^n \quad (22)$$

with the coefficients

$$a_L = \frac{2 - \omega_L^2 \Delta t^2}{1 + \delta_L \Delta t}, \quad (23)$$

$$b_L = -\frac{1 - \delta_L \Delta t}{1 + \delta_L \Delta t}, \quad (24)$$

$$c_L = \frac{\epsilon_0 \Delta\epsilon_L \omega_L^2 \Delta t^2}{1 + \delta_L \Delta t}. \quad (25)$$

The instantaneous Kerr nonlinearity is given by

$$P_K^{n+1} = \epsilon_0 \chi_0^{(3)} (E^{n+1})^3. \quad (26)$$

The Raman effect is a retarded dispersive nonlinear process, which is modeled under the so-called Born-Oppenheimer approximation [13] by

$$\begin{aligned} P_R(t) &= \epsilon_0 E(t) \int_0^t \chi_R^{(3)}(t-t') E^2(t') dt' \\ &= \epsilon_0 E(t) [\chi_R^{(3)}(t) * E^2(t)], \end{aligned} \quad (27)$$

where $\chi_R^{(3)}(t)$ is a time response function of dumped harmonic oscillation

$$\chi_R^{(3)}(t) = \chi_0^{(3)} \exp(-t/\tau_2) \sin(t/\tau_1) u(t), \quad (28)$$

and “*” denotes the convolution integral. This is discretized by introducing an auxiliary variable S as

$$S^{n+1} = a_R S^n + b_R S^{n-1} + c_R (E^n)^2 \quad (29)$$

with

$$a_R = \frac{2 - \omega_R^2 \Delta t^2}{1 + \delta_R \Delta t}, \quad (30)$$

$$b_R = -\frac{1 - \delta_R \Delta t}{1 + \delta_R \Delta t}, \quad (31)$$

$$c_R = \frac{(1 - \alpha) \chi_0^{(3)} \omega_R^2 \Delta t^2}{1 + \delta_R \Delta t}, \quad (32)$$

where ω_R is the oscillating frequency and δ_R the dumping factor of the Raman effect, and finally followed by

$$P_R^{n+1} = \epsilon_0 E^{n+1} S^{n+1}. \quad (33)$$

III. NUMERICAL EXPERIMENT

We have modeled the instantaneous Kerr nonlinearity and the Lorentz linear dispersion. The absorption of an electromagnetic pulse in the nonlinear dispersive media has been investigated for 5 to 50 layers of the APML. The material parameters and the calculation conditions are identical to those in [8] except that the high-order FDTD scheme based on the biorthogonal interpolating scaling function of 10th order (DD₁₀) has been applied [9]; this scheme corresponds in numerical dispersion to approximately the 10th to 14th-order FDTD derived by the Taylor series expansion. The APML is terminated by a perfect electric conductor (PEC) wall implemented by mirroring the field coefficients.

The space step has been chosen to be $\Delta x = \Delta z = 0.0125 \mu\text{m}$ for the standard FDTD and $\Delta x = \Delta z = 0.05 \mu\text{m}$ for the DD₁₀ scheme. The absorption has been evaluated by detecting a relative local error in the analysis region shown in Fig. 1. In order to save the computational region, the boundary conditions are set to be the perfect magnetic conductor (PMC) walls at $x = z = 0 \mu\text{m}$, and the interface between the real domain and the PML has been placed at $x = z = 2.5 \mu\text{m}$. The APML conductance has fourth-order polynomial grading with the maximum value of $\sigma_{max} = 1/(30\pi\sqrt{\epsilon_\infty \Delta x})$ [14].

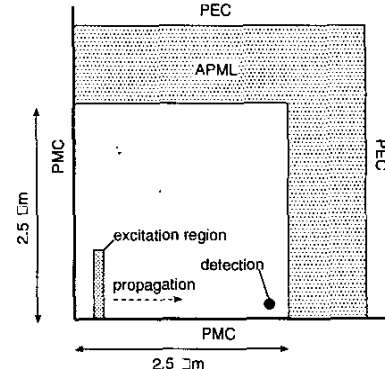


Fig. 1. The analysis region to evaluate the local reflection error.

The carrier frequency of the excitation pulse is 231 THz, i.e. the free-space wavelength is $\lambda_0 = 1.3 \mu\text{m}$; the time envelope is a raised cosine function having approximately 10 carrier cycles in it, which corresponds to the -20 dB bandwidth of approximately 80 THz. The transverse profile of the pulse is a hyperbolic secant function with its full width at half magnitude (FWHM) of 0.65 μm . The media has a instantaneous Kerr nonlinearity of $\chi_0^{(3)} = 2.0 \times 10^{-20} \text{ m}^2/\text{V}^2$, and a linear Lorentz dispersion of $\omega_p = 9.0 \times 10^{14} \text{ rad/s}$, $\delta_p = 5.0 \times 10^9 \text{ 1/s}$, $\Delta\epsilon_p = 3.0$, and $\epsilon_\infty = 6.05$.

With this choice, the numerical dispersion is sufficiently small compared to the Lorentz dispersion, and the carrier frequency is in the range of anomalous dispersion of the Lorentz media; the group velocity dispersion parameter β_2

ranges from -100 to -5 ps^2/m over the bandwidth from 190 to 270 THz , where temporal soliton pulse can be formed by an excitation with sufficient intensity, i.e. 7×10^9 V/m . The reference structure has $7.5 \mu\text{m} \times 7.5 \mu\text{m}$ region terminated with perfect electric conductor (PEC) walls instead of PML.

The resulting frequency responses of the absorption are plotted in Fig. 2 for the standard FDTD and for the DD₁₀ scheme. It is demonstrated in the results that the absorption improves as the number of layers increases to as large as 50 for the high-order scheme, while only marginal improvement is observed for the standard FDTD. Preliminary experiments have shown that the standard FDTD exhibits -70 dB absorption with 10 layers for the weaker nonlinearity of less initial pulse amplitude 2×10^9 V/m , and less than -100 dB for linear media.

For the DD₁₀ scheme, due to the small numerical dispersion error, the cell size is four times larger than that for the FDTD, so is the actual thickness of the APML, while the number of layers is the same; in other words, the 50 APML for the DD₁₀ scheme corresponds in thickness to a 200 APML for the FDTD. Thus the thicker APML have avoided reflection of the highly nonlinear pulse in the DD₁₀ scheme.

IV. CONCLUSION

Larger improvement has been observed in the absorption of the nonlinear dispersive wave for the high-order FDTD scheme than for the standard FDTD. Significantly thick layers are required for better absorption of such a highly nonlinear wave. This fact implies that there still exists some possibility of optimizing the APML parameters to achieve better absorption.

ACKNOWLEDGEMENT

The authors wish to acknowledge the Humboldt Foundation, Germany, for the research fellowship provided to M. Fujii, and the Deutsche Forschungsgemeinschaft and NSF CAREER Award for the sponsorship to the summer research stay of M. Tentzeris at the University of Technology Munich.

REFERENCES

- [1] D.M.Sullivan, "Nonlinear FDTD formulations using z-transforms", *IEEE Trans. Microwave Theory Tech.*, vol. 43, no. 3, pp. 676-682, Mar. 1995.
- [2] D.M.Sullivan, J.Liu, and M.Kuzyk, "Three-dimensional optical pulse simulation using the FDTD method", *IEEE Trans. Microwave Theory Tech.*, vol. 48, no. 7, pp. 1127-1133, July 2000.
- [3] P.M.Goorjian, A.Taflove, R.M.Joseph, and S.C.Hagness, "Computational modeling of femtosecond optical solitons from Maxwell's equations", *IEEE J. Quantum Elec.*, vol. 28, no. 10, pp. 2416-2422, Oct. 1992.
- [4] R.M.Joseph, P.M.Goorjian, and A.Taflove, "Direct time integration of Maxwell's equations in two-dimensional dielectric waveguides for propagation and scattering of femtosecond electromagnetic solitons", *Optics Lett.*, vol. 18, no. 7, pp. 491-493, Apr. 1993.
- [5] P.M.Goorjian and Y.Silberberg, "Numerical simulations of light bullets using the full-vector time-dependent nonlinear Maxwell equations", *J. Opt. Soc. Am. B*, vol. 14, no. 11, pp. 3253-3260, 1997.
- [6] M.Okoniewski, M.Mrozowski, and M.A.Stuchly, "Simple treatment of multi-term dispersion in FDTD", *IEEE Microwave Guided Wave Lett.*, vol. 7, no. 5, pp. 121-123, May 1997.
- [7] A.Taflove and S.C.Hagness, *Computational electrodynamics: the finite-difference time-domain method*, -2nd ed., Artech House, 2000.
- [8] M.Fujii and P.Russer, "A nonlinear and dispersive APML ABC for the FD-TD methods", *IEEE Microwave and Wireless Components Lett.*, vol. 12, no. 11, pp. 444, November 2002.
- [9] M.Fujii and W.J.R.Hoefer, "Application of biorthonormal interpolating wavelets to the Galerkin scheme of time dependent Maxwell's equations", *IEEE Microwave and Wireless Components Lett.*, vol. 11, no. 1, pp. 22-24, Jan. 2001.
- [10] K.S.Yee, "Numerical solution of initial boundary value problems involving Maxwell's equation in isotropic media", *IEEE Trans. Antennas Propagation*, vol. 14, no. 5, pp. 302-307, May 1966.
- [11] M.Fujii and W.J.R.Hoefer, "A wavelet formulation of finite difference method: Full vector analysis of optical waveguide junctions", *IEEE Journal of Quantum Electronics*, vol. 37, no. 8, pp. 1015-1029, Aug. 2001.
- [12] E.M.Tentzeris, A.Cangellaris, L.P.B.Katchi, and J.F.Harvey, "Multi-resolution time-domain (MRTD) adaptive schemes using arbitrary resolutions of wavelets", *IEEE MTT Journal*, vol. 50, no. 2, pp. 501-516, Mar. 2002.
- [13] R.W.Hellwarth, "Third-order optical susceptibilities of liquid and solids", *J. Prog. Quantum Electr.*, vol. 5, pp. 1-68, 1977.
- [14] S.D.Gedney, "An anisotropic perfectly matched layer absorbing media for the truncation of FDTD lattices", *IEEE Trans. Antennas and Propagation*, vol. 44, no. 12, pp. 1630-1639, Dec. 1996.

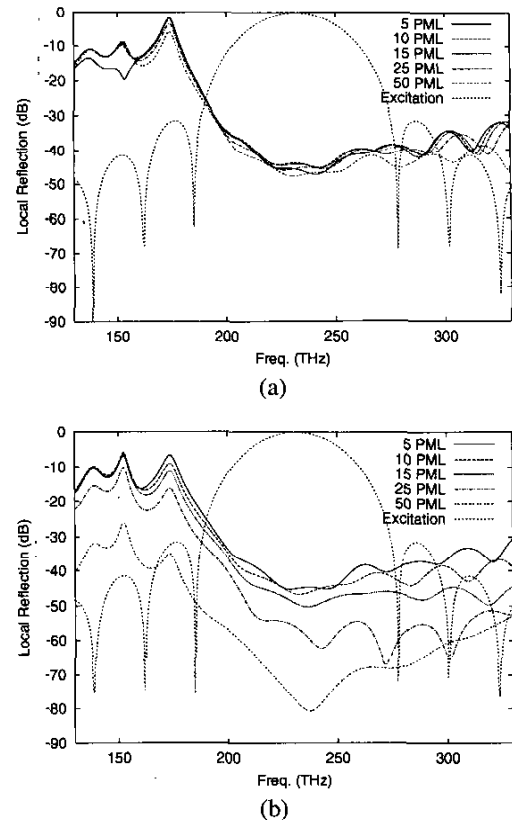


Fig. 2. Relative local reflection: (a) for the standard FDTD, and (b) for the high-order FDTD based on DD₁₀. The excitation spectrum is shown for reference purpose.